Available online at www.sciencedirect.com
ScienceDirect
Polymer 48 (2007) 860–869
polymer
www.elsevier.com/locate/polymer

Largely improved toughness of PP/EPDM blends by adding nano-SiO_2 particles

Hong Yang, Xiaoqing Zhang, Cheng Qu, Bo Li, Lijuan Zhang, Qin Zhang, Qiang Fu*

Department of Polymer Science and Materials, Sichuan University, State Key Laboratory of Polymer Materials Engineering, Chengdu 610065, China

Received 21 September 2006; received in revised form 4 November 2006; accepted 13 December 2006
Available online 20 December 2006

Abstract

As a part of long-term project aimed at super polyolefin blends, in this work, we report the toughness and phase morphology of polypropylene (PP)/EPDM/SiO_2 ternary composites. Two processing methods were employed to prepare PP/elastomer/filler ternary composites. One was called one-step processing method, in which the elastomer and the filler directly melt blended with PP matrix. Another one was called two-step processing method, in which the elastomer and the filler were mixed first, and then melt blended with pure PP. Two kinds of PP (grafted without or with maleic anhydride (PP-*g*-MA)) and SiO_2 (treated with or without coupling agent) were used to control the interfacial interaction among the components. The dependence of the phase morphology on interfacial interaction and processing method was investigated. It was found that the formation of filler-network structure could be a key for a simultaneous enhancement of toughness and modulus of PP and its formation seemed to be dependent on the work of adhesion (W_{AB}) and processing method. As the W_{AB} of PP/EPDM interface was much lower than that of PP/SiO_2 and EPDM/SiO_2, and the two-step processing method was used, the formation of filler-network structure was favorable. In this case, a super toughened PP ternary composite with the Izod impact strength 2–3 times higher than PP/EPDM binary blend and 15–20 times higher than pure PP could be achieved.

Keywords: Ternary composites; Filler-network structure; Work of adhesion

1. Introduction

In the past decade, the use of inorganic filler to improve the physical properties of polymer blends has become widespread in the production of high-performance materials [1–18]. In particular, the fillers can improve the toughness, processibility, heat distortion temperature of polymer blends, and conductive fillers can even make the insulative polymer blend to become a conductive one. Sahnoune et al. [1] have shown that the incorporation of $CaCO_3$ significantly enhanced the stiffness of HDPE/PS blends. Gonzalez and co-workers [2] used $CaCO_3$ particles treated by different coupling agents to modify the mechanical properties of PP/HDPE blends. They found that, due to the particular characteristics of the coupling agents, each treated $CaCO_3$ particles gave rise to increase in a specific mechanical property. Thongruang et al. [3] studied HDPE/UHMWPE/graphite/carbon fiber composites and found that the conductivity increased exponentially with increasing modulus by controlling the distribution of graphite and carbon fiber in HDPE/UHMWPE blends. PEEK composites filled with combining fillers of glass fiber (GF) and mica were also investigated by Gan et al. [4]. The enhanced mechanical strength and reduced coefficient of friction and wearing loss were achieved by replacement of GF with mica, which was owing to the tendency of GF and mica to move and orient in different ways in the process of melt blend and the capability of fine-grained particles locating among the large particles.

Thus, to achieve the best combination of mechanical properties, the key is to control the phase morphology of this ternary polymer composite, especially the distribution and dispersion of the fillers in the polymer blends. The final phase morphology

* Corresponding author. Tel.: +86 28 85405402.
E-mail address: qiangfu@scu.edu.cn (Q. Fu).

0032-3861/$ - see front matter © 2006 Elsevier Ltd. All rights reserved.
doi:10.1016/j.polymer.2006.12.022

of ternary composites is governed by both thermodynamic and kinetic factors, such as interfacial tension, viscosity ratio, shear stress, processing conditions and so on. Several models were developed to predict the phase morphology of ternary composites [18–20]. Gubbels and co-workers [6–8] have done a lot of work on the kinetic and thermodynamic control of the selective localization of carbon black (CB) particles in immiscible PE/PS blends, i.e., in one phase or better at the interface of binary polyblends, so as to decrease the percolation threshold of CB particles in polymers. The results indicated that the minimum electrical resistivity of PE/PS/CB composites corresponded to the preferential localization of CB at the interface. Thus the control and prediction of phase morphology of ternary composites, especially those comprising polymer, elastomer and fillers, are of great importance. Several complex phase morphologies can be formed in such ternary composites, i.e., separated dispersion structure [1,10–18], core–shell structure [10–18] and filler-network structure first reported in our previous publication [16]. Chang and co-workers [10] concluded that the mechanical properties of ternary composites were strongly dependent on microstructure. In their study, the composites with separated dispersion structure showed higher elongation, modulus and impact strength than those of encapsulation structure. However, Jancar and Dibenedetto [11] have shown that the modulus was increased in a condition of separated dispersion while the core–shell microstructure could improve the toughness. In our work, we found that the filler-network structure formed in PP/EPDM/SiO_2 ternary composite led to a simultaneous increase of toughness and strength while both the core–shell structure and separated dispersion structure did not [16]. Up to now, most work has been focused on the relationship between the phase morphology and mechanical properties of such ternary composites [1,9–16], while few attentions have been paid to the thermodynamic and kinetic consideration and prediction of phase morphology of ternary composites [17,18].

In the previous paper [16], we found that, by using different processing methods and adjusting the wettability of nano-SiO_2 particles toward PP and EPDM, three different kinds of phase structures were formed in PP/EPDM/SiO_2 ternary composites. There was separated dispersion structure, core–shell structure, as well as filler-network structure where a large amount of hydrophilic SiO_2 particles agglomerated around EPDM particles and pervaded over the PP matrix. A simultaneous enhancement of toughness and stiffness has been achieved only for PP/EPDM/SiO_2 composites with the filler-network structure. With regard to this, it is essential to study the formation and evolution of the phase morphology in PP/EPDM/SiO_2 ternary composites, especially the formation process of filler-network structure. It is well known that the final phase structure of ternary composites is determined not only by the thermodynamic factor (e.g. interfacial tension), but rather by the kinetic factor (e.g. shear stress and processing conditions). In this study, we will report our efforts to control the phase structure of PP/EPDM/SiO_2 composites by adjusting the interfacial interaction and by using different processing methods, as a long-term project aimed at super polyolefin blends/composites.

2. Experimental

2.1. Materials

The materials used for the preparation of PP/EPDM/SiO_2 and PP-*g*-MA/EPDM/SiO_2 composites are listed in Table 1. Two kinds of PP (grafted without or with maleic anhydride (PP-*g*-MA)) and SiO_2 (treated with or without coupling agent) were used to control the interfacial interaction among the components. Polypropylene (PP), polypropylene grafted with maleic anhydride (PP-*g*-MA), EPDM and fumed nano-SiO_2 particles used in this study were commercially available. The hydrophobic nano-SiO_2 (A-SiO_2) was treated by coupling agent D4 (octamethyl cyclotetrasiloxane) before use while the hydrophilic nano-SiO_2 (B-SiO_2) was received without any pretreatment.

2.2. Sample preparation

Two processing methods were employed to prepare PP/elastomer/filler ternary composites. One was called one-step processing method, in which the elastomer and the filler were directly melt blended with PP matrix. Another one was called two-step processing method, in which the elastomer and the filler were mixed by means of a two-roll mill at room temperature for 10 min to get masterbatch first, and then the masterbatch was melt blended with pure PP. The ratio of PP/EPDM was fixed at 80/20 (wt%/wt%) and the blending

Table 1
Materials

	Materials	Brand	Supplier	Characteristics
	PP	T30s	Du Shan Zi Petroleum Chemical, China	MFI = 2.64 g/10 min (210 °C, 2.16 kg)
	PP-*g*-MA	–	Chenguang Co.	MFI = 6.74 g/10 min (210 °C, 2.16 kg), MA content = 0.9 wt%
	EPDM	EP35	Japan Synthetic Rubber Co. Ltd	PP content: 43%, Mooney viscosity: 83(100 °C), the third monomer: ENB
Fumed nano-SiO_2	Hydrophobic SiO_2 (A-SiO_2)	JT-SQ	Chendu Today Chemical Co., Ltd	Particle size: 10–30 nm, $S_{(BET)} = 200\ m^2/g$
	Hydrophilic SiO_2 (B-SiO_2)	HL-150	Guangzhou GBS High Tech. & Industry Co.	Particle size: 15–20 nm, $S_{(BET)} = 150 \pm 10\ m^2/g$

of several PP/elastomer/filler ternary composites (80/20/x wt%, $x = 1, 3, 5$) was conducted in a two-screw extruder at 140–210 °C, and then injection molded in PS40E5ASE (Japan) at 180–210 °C to obtain standard specimen for mechanical properties' tests.

Melt blending of PP/EPDM/SiO_2 composites was also conducted using a Haake internal mixer set at a barrel temperature of 210 °C, and the rotor speed was 50 r/min. The mixing time varied from 1 to 30 min was recorded under the same processing parameters for comparison.

2.3. Scanning electron microscopic (SEM) experiments

The morphology of the blends was studied by preferential etching of EPDM phase in dimethylbenzene for 2 h. The samples were cryogenically fractured in the direction perpendicular to flow direction in liquid nitrogen before etching. The etched samples were carefully washed several times by using fresh dimethylbenzene, and then with alcohol for three times. The samples were dried under vacuum at room temperature for 24 h. Then the fractured samples were observed in a JEOL JSM-5900LV SEM instrument, using an acceleration voltage of 20 kV, which could show the dispersion of elastomer and filler in PP matrix.

2.4. Contact angle measurements

Contact angles were measured in a sessile drop mold with KRUSS DSA100. PP and EPDM samples for contact angle measurement were compression molded between clean silicon wafers at 210 °C for 3 min and then cooled to 25 °C under pressure for 1 min. SiO_2 powders were compression molded by using a special mold at room temperature under a certain pressure. Contact angles were measured on 3 μl of wetting solvent at 20 °C, and the results reported were the mean values of 10 replicates.

2.5. Dynamic mechanical analysis (DMA)

The dynamic mechanical analysis was carried out using a TA Instruments Q800 DMA. All the samples were measured in a dual cantilever mode over the temperature range of −100 to 100 °C at a heating rate of 3 °C/min and at a frequency of 10 Hz. Specimen dimensions were $40 \times 10 \times 4.2$ mm^3.

2.6. Izod impact strength test

The notched Izod impact strength was used to evaluate the toughness of the samples. The notched specimens were tested with a VJ-40 impact test machine at room temperature, according to GB/T 1834-1996 standard. Each impact test was repeated at least five times, and the results were averaged.

3. Results

3.1. SEM observation

SEM experiment was carried out to understand the phase morphology of ternary composites. In our previous paper [16], three different kinds of phase morphologies were observed in PP/EPDM/SiO_2 ternary composites (as shown in Fig. 1, the dark holes represent the etched EPDM particles).

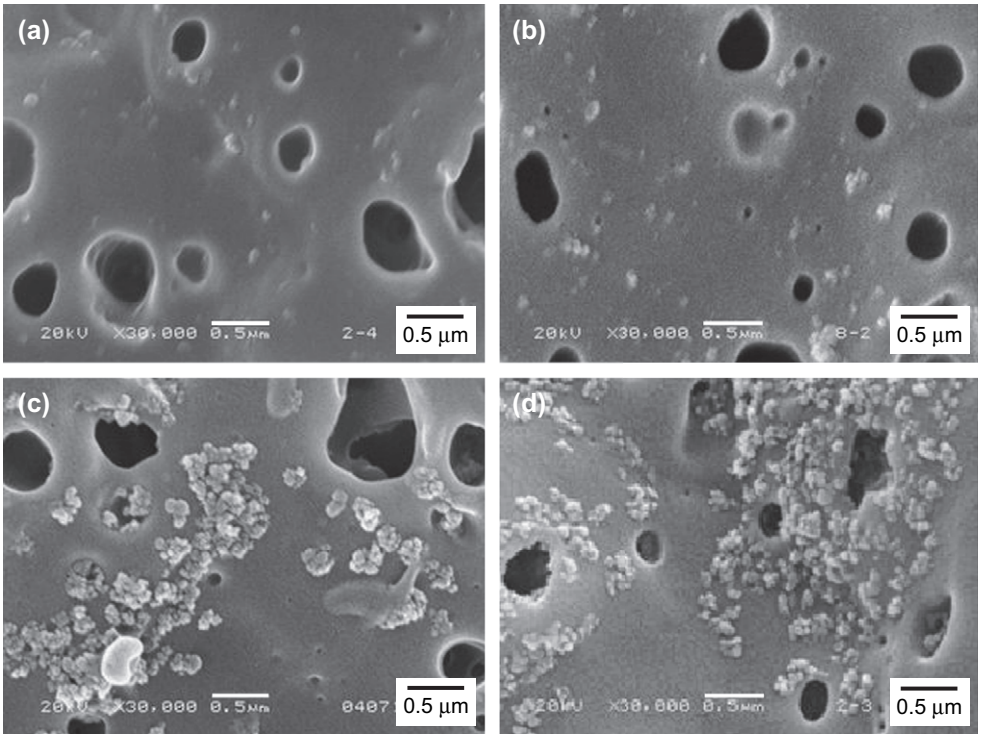

Fig. 1. SEM images of PP/EPDM/nano-SiO_2 (80/20/3) ternary composites: (a) one-step, A-SiO_2; (b) two-step, A-SiO_2; (c) one-step, B-SiO_2; (d) two-step, B-SiO_2 (Ref. [16]).

For PP/EPDM/A-SiO_2 composite prepared by one-step processing method and two-step processing method, a core–shell structure is most likely formed since few A-SiO_2 particles (bright particles) can be seen in PP matrix (seen in Fig. 1(a) and (b)). And in these two cases, smooth interface between PP and EPDM without any A-SiO_2 particles is observed. For PP/EPDM/B-SiO_2 composite prepared by one-step processing method, large aggregates of B-SiO_2 particles with a size of 0.5–1.0 μm exist in PP matrix, indicating that a separated dispersion structure with large B-SiO_2 aggregates is probably formed (Fig. 1(c)). However, the filler-network structure wherein a large amount of B-SiO_2 particles agglomerate around EPDM particles (dark holes) and pervade over the PP matrix is clearly observed in PP/EPDM/B-SiO_2 composite prepared by two-step processing method (Fig. 1(d)).

The similar phase morphology of PP-*g*-MA/EPDM/SiO_2 composites has been observed, as shown in Fig. 2. As can be seen, the core–shell structure is formed in PP-*g*-MA/EPDM/A-SiO_2 composites prepared by two processing methods (Fig. 2(a) and (b)). Smooth interface is also observed and nearly no A-SiO_2 particles are found there as well. In PP-*g*-MA/EPDM/B-SiO_2 composites, separated dispersion structure is formed in ternary composite prepared by one-step processing method (Fig. 2(c)) and filler-network structure is also observed in that prepared by two-step processing method (Fig. 2(d)). The SEM results suggest that phase structure of ternary composites is influenced by the type of SiO_2 particles and processing methods, and two-step processing method favors the formation of filler-network structure in both PP/EPDM/B-SiO_2 and PP-*g*-MA/EPDM/B-SiO_2 composites.

3.2. DMA results

The formation of filler-network structure in PP/EPDM/B-SiO_2 (PP-*g*-MA/EPDM/B-SiO_2) composites can also be confirmed by DMA technique. Fig. 3 depicts the temperature dependence of tan δ at 10 Hz for PP/EPDM (80/20) binary blend and PP/EPDM/B-SiO_2 (80/20/5) ternary composite. Two tan δ peaks correspond to the glass transition temperatures (T_g) of PP and EPDM. The glass transition temperatures (T_g) and the peak value of PP and EPDM are listed in Table 2. The relative increment of peak value (ΔP_r) can be calculated from the peak value by Eq. (1):

$$\Delta P_r = \frac{|P_{T5} - P_B|}{P_B} \times 100\% \quad (1)$$

where P_B represents the peak value of PP/EPDM (80/20) binary blend and P_{T5} represents the peak value of PP/EPDM/B-SiO_2 (80/20/5) ternary composite. As we know, the peak value is proportional to the concentration of the component in the composition. In PP/EPDM/B-SiO_2 composite prepared by one-step processing method, ΔP_r of PP is larger than that of EPDM. This indicates that B-SiO_2 particles are mainly dispersed in PP matrix, thus increasing the effective volume of PP. And this can be further confirmed by the larger increase of T_g of PP (from 16.7 °C to 20.0 °C) than that of EPDM (from −34.9 °C to −32.5 °C), owing to the influence of B-SiO_2 particles on the mobility of PP and EPDM chains. Therefore, separated dispersion structure is formed in this composite. In PP/EPDM/B-SiO_2 composite prepared by

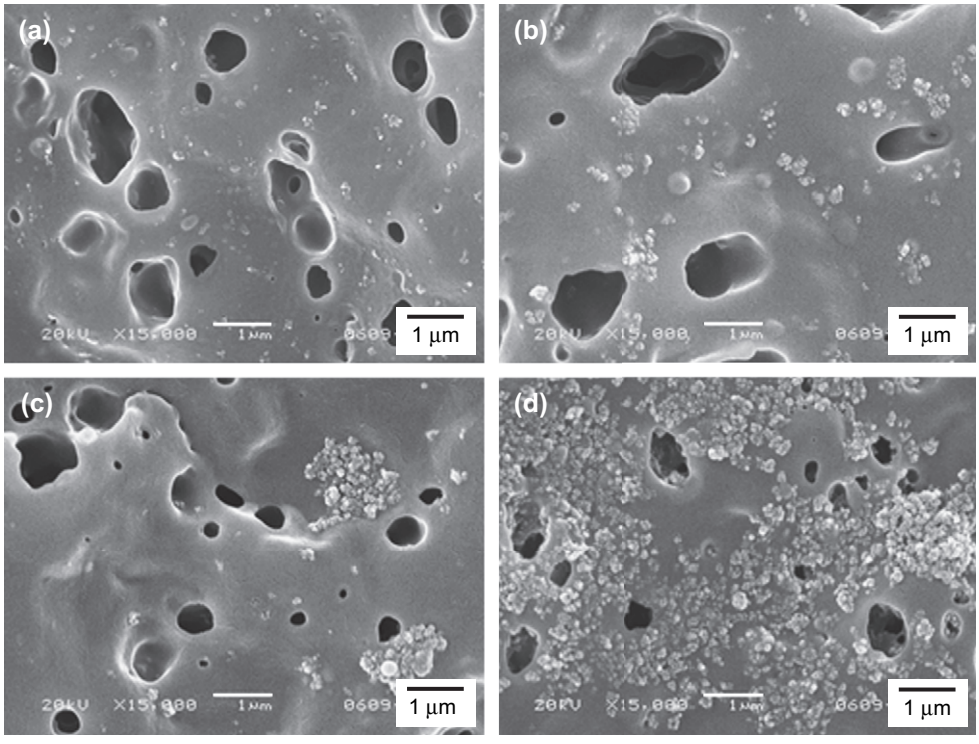

Fig. 2. SEM images of PP-*g*-MA/EPDM/nano-SiO_2 (80/20/3) ternary composites: (a) one-step, A-SiO_2; (b) two-step, A-SiO_2; (c) one-step, B-SiO_2; (d) two-step, B-SiO_2.

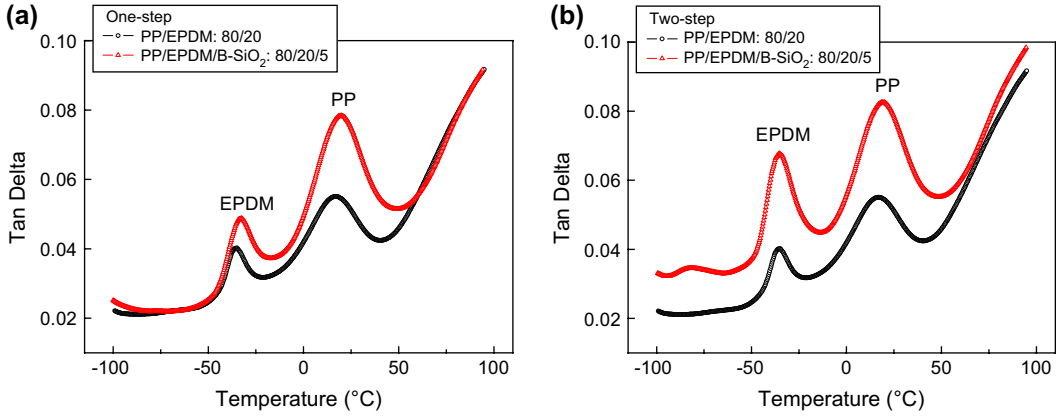

Fig. 3. Temperature dependency of tan δ at 10 Hz for PP/EPDM (80/20) binary blend and PP/EPDM/B-SiO_2 (80/20/5) composite: (a) one-step; (b) two-step.

Table 2
The glass transition temperature (T_g), peak value and relative increment of peak value (ΔP_r) of PP and EPDM in PP/EPDM (80/20) binary blend and PP/EPDM/B-SiO_2 (80/20/5) ternary composite

Sample	Processing method	Tan δ (°C)		Peak value		ΔP_r (%)	
		PP	EPDM	PP	EPDM	PP	EPDM
PP/EPDM (80/20)		16.7	−34.9	0.055	0.040	–	–
PP/EPDM/B-SiO_2 (80/20/5)	One-step	20.0	−32.5	0.078	0.049	41.8	22.5
	Two-step	18.5	−35.5	0.083	0.068	50.9	70.0

two-step processing method, ΔP_r of EPDM is larger than that of PP. Meanwhile, T_g of PP is increased from 16.7 °C to 18.5 °C but that of EPDM almost keeps constant. This can be only explained that B-SiO_2 particles are seldom dispersed in EPDM phase, but rather most of them are concentrated around EPDM phase, resulting in the increase of the effective volume of EPDM, and at the same time, B-SiO_2 particles pervade over PP matrix, effectively decreasing the mobility of PP chains. So it can be concluded that the filler-network structure with a large amount of B-SiO_2 particles agglomerated around EPDM particles and pervading over PP matrix is essentially formed in this composite [16].

3.3. Izod impact strength

Polypropylene (PP) is one of the most important commodity polymers. It is widely used in automobile, household appliance and construction industry due to its balanced mechanical properties. The application of PP, however, is limited by its brittleness, especially at low temperature, as well as low stiffness at elevated temperature. In order to improve the impact toughness of PP and extend its application range, a lot of extensive and thorough researches on PP toughened with different particles (including both rubber and rigid particles) have been made. More than 10 times' increase of Izod impact strength has been reported for PP/EPDM binary blends at the brittle–ductile transition [16,23]. We found that the toughness of PP/EPDM blends could be further improved by adding nano-SiO_2 particles [16]. The change of Izod impact strength as a function of nano-SiO_2 content for PP-*g*-MA/EPDM/SiO_2 composites prepared by two processing methods is shown in Fig. 4. It is very interesting to see that, the Izod impact strength of the ternary composite, prepared by two-step processing method and by using non-surface treated hydrophilic nano-SiO_2 particles (B-SiO_2), is remarkably enhanced. In this case, a super toughened PP-*g*-MA ternary composite with Izod impact strength 2–3 times higher than PP-*g*-MA/EPDM binary blends and 15–20 times higher than pure PP-*g*-MA has been achieved by adding 3–5 wt% B-SiO_2 particles. For the other three composites, however, not much

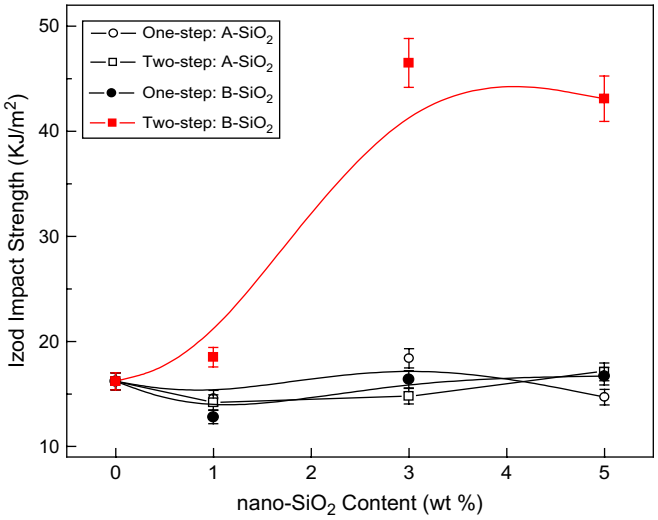

Fig. 4. Izod impact strength versus nano-SiO_2 content for different PP-*g*-MA/EPDM/SiO_2 composites prepared by two processing methods (PP-*g*-MA/EPDM = 80/20).

increase of Izod impact strength is observed. This result is consistent with that in PP/EPDM/SiO_2 composites reported in our previous paper (seen in Ref. [16], Fig. 3). Since a possible filler-network structure is only seen in the composites prepared by two-step processing method and by using B-SiO_2, this result indicates that a largely improved toughness in PP/EPDM/SiO_2 ternary composites can be only resulted from the special phase structure. This also explains, at least in part, that not much report on the simultaneous enhancement of toughness and modulus of polymer/elastomer/filler ternary composites can be found in literature.

4. Discussions

4.1. Interfacial tension

It seems that there exists a remarkable parallelism between the toughness and the phase morphology. In order to study the formation and evolution of phase structure, both thermodynamic and kinetic considerations should be taken into account to understand the distribution of SiO_2 particles in PP/EPDM/SiO_2 ternary composites during mixing. Let us first discuss the interfacial tension. The contact angles with water and diiodomethane are listed in Table 3. Then, the surface tension, dispersion and polar components of the materials can be estimated from the contact angle data by using the following two equations (Eq. (2) for water and Eq. (3) for diiodomethane) according to Wu:

$$(1+\cos\theta_{H_2O})\gamma_{H_2O} = 4\left(\frac{\gamma^d_{H_2O}\gamma^d}{\gamma^d_{H_2O}+\gamma^d}+\frac{\gamma^p_{H_2O}\gamma^p}{\gamma^p_{H_2O}+\gamma^p}\right) \quad (2)$$

$$(1+\cos\theta_{CH_2I_2})\gamma_{CH_2I_2} = 4\left(\frac{\gamma^d_{CH_2I_2}\gamma^d}{\gamma^d_{CH_2I_2}+\gamma^d}+\frac{\gamma^p_{CH_2I_2}\gamma^p}{\gamma^p_{CH_2I_2}+\gamma^p}\right) \quad (3)$$

in which $\gamma = \gamma^d + \gamma^p$, $\gamma_{H_2O} = \gamma^d_{H_2O} + \gamma^p_{H_2O}$, $\gamma_{CH_2I_2} = \gamma^d_{CH_2I_2} + \gamma^p_{CH_2I_2}$, γ is surface tension, d is dispersion component and p is polar component, θ_{H_2O} and $\theta_{CH_2I_2}$ are contact angles of the polymer with water and diiodomethane, respectively. The numerical values used are $\gamma^d_{H_2O} = 22.1$ dyn/cm, $\gamma^p_{H_2O} = 50.7$ dyn/cm, $\gamma^d_{CH_2I_2} = 44.1$ dyn/cm, $\gamma^p_{CH_2I_2} = 6.7$ dyn/cm. The values of surface tension, dispersion and polar components are also listed in Table 3. And then the interfacial tension of each pairs can be calculated from surface tension by using the geometric mean equation of Wu [21]:

Table 3
Contact angle and surface tension results of PP, EPDM and SiO_2 particles

Sample	Contact angle (°)		Surface tension (mN/m)		
	Water	Diiodomethane	Total (γ)	Dispersion component (γ^d)	Polar component (γ^p)
PP	95.2	39.7	40.04	39.79	0.26
PP-*g*-MA	106.5	59.7	29.30	29.29	0.01
EPDM	100.8	57.0	30.43	30.13	0.30
A-SiO_2	140.6	79.5	24.14	20.82	3.32
B-SiO_2	10.1	22.4	74.10	35.24	38.86

$$\gamma_{AB} = \gamma_A + \gamma_B - 2\left(\gamma^d_A\gamma^d_B\right)^{1/2} - 2\left(\gamma^p_A\gamma^p_B\right)^{1/2} \quad (4)$$

where γ_{AB} is the interfacial tension, γ_A and γ_B are the surface tensions of the two materials in contact. In PP/EPDM/SiO_2 composites and PP-*g*-MA/EPDM/SiO_2 composites of this study, three different interfaces are probably formed – PP/EPDM, PP/SiO_2, EPDM/SiO_2 in the former and PP-*g*-MA/EPDM, PP-*g*-MA/SiO_2, EPDM/SiO_2 in the latter. The calculated interfacial tensions of all possible polymer/elastomer, polymer/filler and elastomer/filler pairs are given in Tables 4 and 5.

A study of the interfacial tension data indicates that, in PP/EPDM/A-SiO_2 composite, the interfacial tension of PP/A-SiO_2 is greater than that of EPDM/A-SiO_2. Based on the concept that the phase morphology of a multicomponent polymer system will be that which has the lowest free energy, it is most likely that, in this system, the structure of A-SiO_2 particles is encapsulated by EPDM and the final phase morphology will be core–shell structure. In PP/EPDM/B-SiO_2 composite, however, the interfacial tensions of PP/B-SiO_2 and EPDM/B-SiO_2 are similar. This means that both PP and EPDM have similar tendency to encapsulate B-SiO_2 particles, thus the final phase structure of this composite should be the separated dispersion structure. Applying this criteria to PP-*g*-MA/EPDM/SiO_2 composites, it can be predicted that the final phase structure should be the core–shell structure both in PP-*g*-MA/EPDM/A-SiO_2 composite and PP-*g*-MA/EPDM/B-SiO_2 composite.

4.2. Work of adhesion

From the interfacial tension data, one cannot predict the formation of filler-network structure. SEM results discussed in the previous section have illustrated the possible filler-network structure in PP/EPDM/B-SiO_2 and PP-*g*-MA/EPDM/B-SiO_2 composites prepared by two-step processing method.

Table 4
The value of interfacial tension (γ_{AB}) of PP/EPDM/SiO_2 composites

System	Possible pairs	Interfacial tension (γ_{AB}) (mN/m)	Final phase structure
PP/EPDM/A-SiO_2	PP/EPDM	0.662	Core–shell
	PP/A-SiO_2	4.757	
	EPDM/A-SiO_2	2.482	
PP/EPDM/B-SiO_2	PP/EPDM	0.662	Separated dispersion
	PP/B-SiO_2	32.891	
	EPDM/B-SiO_2	32.531	

Table 5
The value of interfacial tension (γ_{AB}) of PP-*g*-MA/EPDM/SiO_2 composites

System	Possible pairs	Interfacial tension (γ_{AB}) (mN/m)	Final phase structure
PP-*g*-MA/EPDM/A-SiO_2	PP-*g*-MA/EPDM	0.206	Core–shell
	PP-*g*-MA/A-SiO_2	3.687	
	EPDM/A-SiO_2	2.482	
PP-*g*-MA/EPDM/B-SiO_2	PP-*g*-MA/EPDM	0.206	Core–shell
	PP-*g*-MA/B-SiO_2	37.898	
	EPDM/B-SiO_2	32.531	

In order to explain this, thermodynamic work of adhesion (W_{AB}) is employed here. It can be calculated using the following equation [22]:

$$W_{AB} = 2\left(\gamma_A^d \gamma_B^d\right)^{1/2} + 2\left(\gamma_A^p \gamma_B^p\right)^{1/2} \quad (5)$$

The results are summarized in Table 6 (PP/EPDM/SiO_2 composites) and Table 7 (PP-*g*-MA/EPDM/SiO_2 composites). The higher value of W_{AB} reflects a strong interaction between two components, thus such interface will be relatively more stable under the shear forces during mixing. Taking PP/EPDM/SiO_2 composites as examples, we discuss the possible criteria for the formation of filler-network structure in polymer/elstomer/filler ternary composites. For PP/EPDM/A-SiO_2 composite, W_{AB} of PP/EPDM interface is much higher than that of PP/A-SiO_2 and EPDM/A-SiO_2 interfaces. This demonstrates that, compared with PP/A-SiO_2 and EPDM/A-SiO_2, PP/EPDM interface is much more stable and cannot be destroyed under the same shear forces. Meanwhile, the surface treatment of A-SiO_2 particles significantly decreases the interfacial tension of PP/A-SiO_2 and EPDM/A-SiO_2 compared with B-SiO_2 (untreated) (seen in Table 4), indicating good adhesion between PP and A-SiO_2 and between EPDM and A-SiO_2. Thus, A-SiO_2 particles more likely exist in PP or EPDM but not at the interphase between PP and EPDM. Since the final phase structure of PP/EPDM/A-SiO_2 composite is the core–shell structure, most of A-SiO_2 particles are encapsulated in EPDM phase. This is in good agreement with SEM results. For PP/EPDM/B-SiO_2 composite, however, W_{AB} of PP/EPDM interface is much lower than that of PP/B-SiO_2 and EPDM/B-SiO_2. This means that PP/EPDM interface can easily be destroyed in comparison with PP/B-SiO_2 and EPDM/B-SiO_2 interfaces. Meanwhile, poor adhesion of B-SiO_2 particles with PP and EPDM is expected because of the comparatively higher interfacial tension values of PP/B-SiO_2 and EPDM/B-SiO_2, which make B-SiO_2 particles effectively migrate from one phase to another phase. In this case, the interface of PP/EPDM, which can be comparatively easily destroyed, tends to block the B-SiO_2 particles' transfer, thus making their temporary accumulation around EPDM particles. Therefore, the comparatively weak thermodynamic work of adhesion provides a possibility to form filler-network structure. The similar conclusion can also be drawn in PP-*g*-MA/EPDM/SiO_2 ternary composites.

Table 6
The value of work of adhesion (W_{AB}) of PP/EPDM/SiO_2 composites

System	Possible pairs	Work of adhesion (W_{AB}) (mN/m)
PP/EPDM/A-SiO_2	PP/EPDM	69.81
	PP/A-SiO_2	59.42
	EPDM/A-SiO_2	52.09
PP/EPDM/B-SiO_2	PP/EPDM	69.81
	PP/B-SiO_2	81.25
	EPDM/B-SiO_2	72.00

Table 7
The value of work of adhesion (W_{AB}) of PP-*g*-MA/EPDM/SiO_2 composites

System	Possible pairs	Work of adhesion (W_{AB}) (mN/m)
PP-*g*-MA/EPDM/A-SiO_2	PP-*g*-MA/EPDM	59.52
	PP-*g*-MA/A-SiO_2	49.75
	EPDM/A-SiO_2	52.09
PP-*g*-MA/EPDM/B-SiO_2	PP-*g*-MA/EPDM	59.52
	PP-*g*-MA/B-SiO_2	65.50
	EPDM/B-SiO_2	72.00

4.3. Effect of processing methods and mixing time

According to the interfacial tension results, the final phase structure of PP/EPDM/B-SiO_2 composite is separated dispersion structure and that of PP-*g*-MA/EPDM/B-SiO_2 composite is core–shell structure. However, for polymer system, the kinetics plays an even more important role in the final phase structure. Shear forces and rheology of each polymer phase can result in the migration of B-SiO_2 particles from one phase to the second one. For PP/EPDM/B-SiO_2 composite prepared by one-step processing method, B-SiO_2 particles are randomly dispersed in PP and EPDM phases at the very beginning of mixing. Because of the lower viscosity and higher concentration of PP in the composition, most of B-SiO_2 particles likely exist in PP matrix. Thus, the separated dispersion structure with large B-SiO_2 aggregates existing in PP matrix is observed. For PP/EPDM/B-SiO_2 composite prepared by two-step processing method, B-SiO_2 particles are first dispersed in EPDM phase. Upon the addition and melting of PP, B-SiO_2 particles effectively migrate from the higher melt viscosity phase (EPDM) to the lower melt viscosity phase (PP) because of the poor adhesion of B-SiO_2 between PP and EPDM. Additionally, since PP/EPDM interface of this system is not stable and can be easily destroyed, B-SiO_2 particles tend to move into the interphase between PP and EPDM, and finally a large amount of B-SiO_2 particles accumulate around EPDM particles. It can be concluded that two-step processing method is in favor of the formation of the filler-network structure.

This can be also confirmed by investigating the evolution of the phase morphology of PP/EPDM/B-SiO_2 composites with mixing time. The development of phase structure of PP/EPDM/B-SiO_2 (80/20/3) composite prepared by two processing methods is shown in Fig. 5. Originally, B-SiO_2 particles are randomly dispersed in PP and EPDM phases in PP/EPDM/B-SiO_2 composite prepared by one-step processing method, and are first encapsulated in EPDM phase in PP/EPDM/B-SiO_2 composite prepared by two-step processing method. After 10 min of mixing, many large B-SiO_2 aggregates are found in PP matrix in the former (Fig. 5(a1)) and few B-SiO_2 particles are finely dispersed in the vicinity of the etched EPDM phase in the latter (Fig. 5(b1)). With the increase of mixing time, B-SiO_2 particles keep migrating from one phase to another. For PP/EPDM/B-SiO_2 composite prepared by two-step processing method, a majority of B-SiO_2 particles are forced out from EPDM phase, and tend to accumulate around EPDM particles. After 20 min, a large amount of

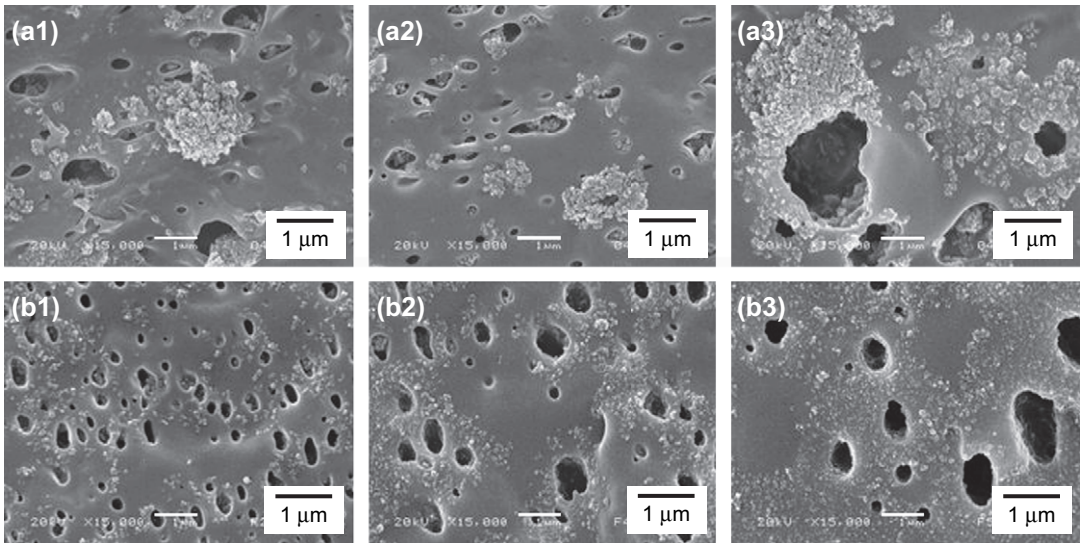

Fig. 5. Phase structures of PP/EPDM/B-SiO_2 (80/20/3) composites at different mixing times: (a) one-step; (b) two-step; (1) 10 min; (2) 20 min; (3) 30 min.

B-SiO_2 particles concentrated around EPDM particles and pervading over the PP matrix are clearly observed in PP/EPDM/B-SiO_2 composite prepared by two-step processing method (Fig. 5(b2)). In another words, filler-network structure is expectedly formed at this time of mixing. However, this filler-network structure is only observed in PP/EPDM/B-SiO_2 composite prepared by one-step processing method after a longer mixing (30 min), seen in Fig. 5(a3). Indeed, the weak thermodynamic work of adhesion of PP/EPDM in comparison with that of PP/B-SiO_2 and EPDM/B-SiO_2 (i.e., $W_{PP/EPDM} < W_{PP/B\text{-}SiO_2}$ and $W_{EPDM/B\text{-}SiO_2}$) is essential for the temporary accumulation of B-SiO_2 particles around EPDM particles. Since B-SiO_2 particles are first dispersed in EPDM phase and then melt blended with PP, the effective mixing time of two-step processing method is much longer compared with that of one-step processing method, which explains a delay in the formation of the filler-network structure in PP/EPDM/B-SiO_2 composite prepared by one-step processing method. Due to the limit of practical mixing time, filler-network structure can be effectively formed and frozen by crystallization of PP just in PP/EPDM/B-SiO_2 composite prepared by two-step processing method.

4.4. Toughening mechanism

According to the framework of Wu's theory [24–28], for polymer/rubber binary blend, a sharp brittle–ductile transition occurred at a critical surface-to-surface interparticle distance, or the critical matrix-ligament thickness τ_c [25].

$$\tau_c = d_c\left[(\pi/6\phi_r)^{1/3} - 1\right] \tag{6}$$

where d_c was the critical rubber particle diameter, ϕ_r was the rubber volume fraction, τ represented the average surface-to-surface interparticle distance (i.e., the average matrix-ligament thickness) and depended on the rubber volume fraction. If $\tau < \tau_c$, the continuum percolation of stress volume around rubber particles would occur; the matrix yielding would propagate and pervade over the entire matrix, and then the blend would be tough. On the contrary, if $\tau > \tau_c$, the matrix yielding could not propagate, and the blend failed in a brittle manner. For PP/EPDM/B-SiO_2 ternary composite prepared by two-step processing method, since large amount of B-SiO_2 particles closely aggregate around EPDM particles, these SiO_2-surrounded EPDM particles can be regarded as a soft core surrounded by rigid SiO_2 particles' shell of comparable size. This structure increases the effective volume of the rubber particles, thus effectively decreasing the interparticle distance (τ). Besides, the stress fields around SiO_2 particle can interfere or overlap with those around the EPDM particles when EPDM particles are closely surrounded by SiO_2 particles and a percolation of SiO_2 particles in PP matrix is formed. In this case, the stress fields around SiO_2 particles seem to serve as a bridge between two neighboring rubber particles. Therefore, the synergic effect between the decrease of the interparticle distance and the overlap of the stress field between EPDM and SiO_2 particles is believed to result in the observed increase of Izod impact strength in PP/EPDM/B-SiO_2 ternary composites with 20 wt% EPDM content. The schematic representation is shown in Fig. 6. The impact-fractured surface of PP/EPDM composite with and without B-SiO_2 particles provides a better understanding of the toughening effect of this filler-network structure (seen in Fig. 7). For PP/EPDM (80/20) binary blend, a large number of microvoids formed during the fracture process caused by the debonding of EPDM particles from the matrix and a relative flat surface without any considerable plastic deformation of the ligaments are observed in Fig. 7(a) and (a′), which means that the system undergoes a brittle failure process. After adding 5 wt% B-SiO_2 particles, one observes a rough impact-fractured surface (Fig. 7(b)). Many tick and long strips which are perpendicular to the impact fracture direction can be clearly seen at high magnification (Fig. 7(b′)). This

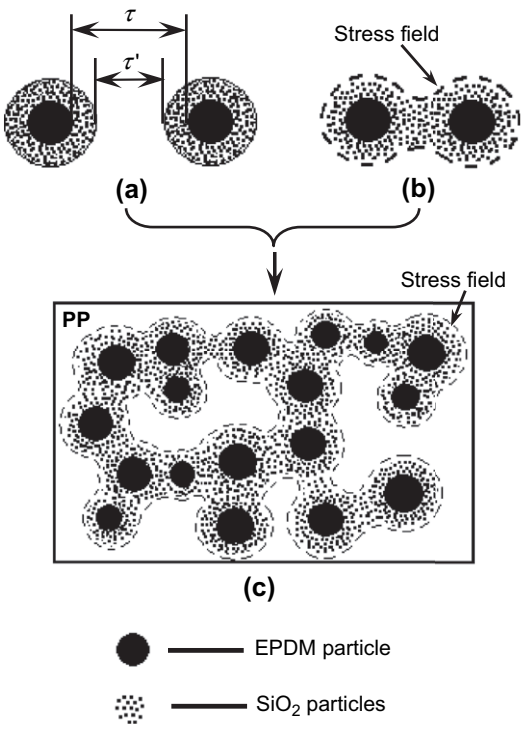

Fig. 6. The schematic representation of toughening effect of B-SiO_2 particles on PP/EPDM binary blend: (a) decreasing of τ; (b) overlap of stress field; (c) percolation of the stress field in the entire PP matrix.

indicates that the formation of the filler-network effectively stops the further development of the crazes and makes the propagation of the crazes into the direction perpendicular to the impact fracture direction, thus enables the sample to sustain a higher loading. Also, it is easy to understand the way that the core–shell phase structure obtained in PP/EPDM/A-SiO_2 composites, or a separated dispersion structure with aggregated SiO_2 particles obtained in PP/EPDM/B-SiO_2 composites prepared by one-step processing method, cannot achieve a remarkable increase of Izod impact strength. For the core–shell phase structure with SiO_2 particles encapsulated by EPDM, just only a slight increase of the effective volume fraction of EPDM dispersed phases is achieved, which is of little avail to the improvement of Izod impact strength. For the separated dispersion structure with aggregated SiO_2 particles, large SiO_2 aggregates existing in PP matrix act as stress concentrations so that they cannot interact with the stress fields around EPDM particles effectively.

5. Conclusions

Three kinds of phase structures are clearly observed in both PP/EPDM/SiO_2 and PP-*g*-MA/EPDM/SiO_2 ternary composites prepared by two processing methods and using two kinds of SiO_2 particles. However, the filler-network structure, which can be further confirmed by DMA results, is formed only in

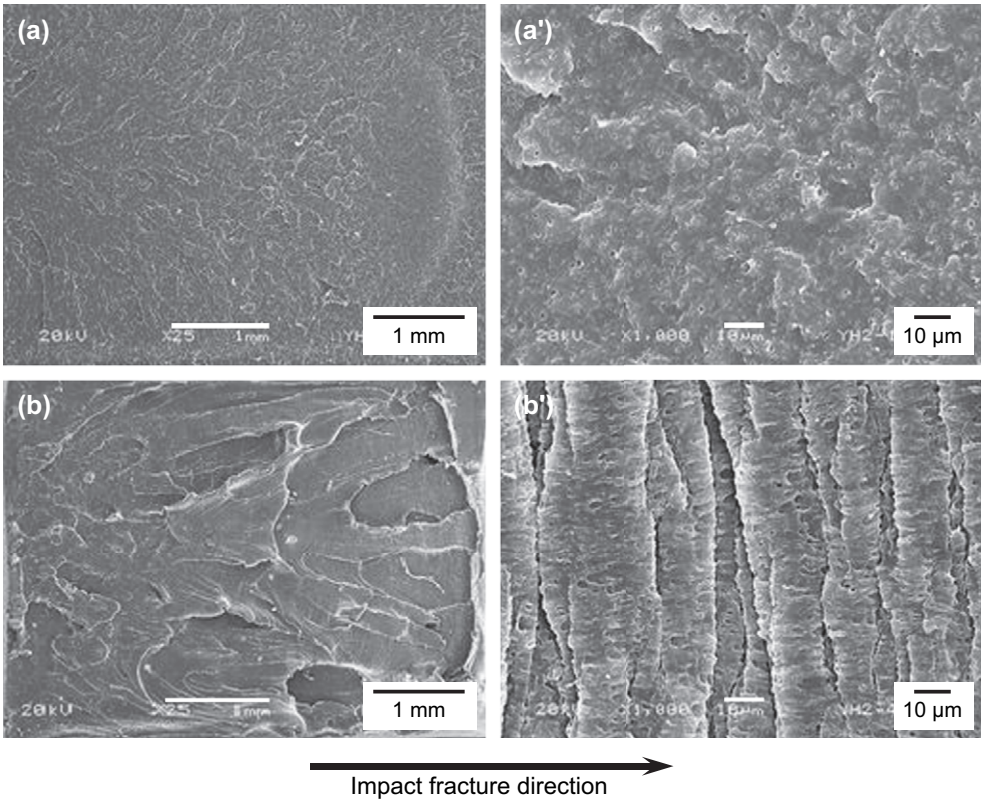

Fig. 7. SEM images of impact-fractured surface of (a) PP/EPDM (80/20) binary blend and (b) PP/EPDM/B-SiO_2 (80/20/5) ternary composite prepared by two-step processing method. (a)(b) Low magnification; (a′)(b′) high magnification.

PP/EPDM/B-BiO_2 and PP-*g*-MA/EPDM/B-BiO_2 composites prepared by two-step processing method. Consequently, the Izod impact strength of both composites is significantly increased with the B-SiO_2 content. The formation of the filler-network structure is mainly controlled by the following factors: (1) the poor adhesion of B-SiO_2 particles with PP and EPDM, according to the value of interfacial tension, makes B-SiO_2 particles effectively migrate from one phase to the second phase; (2) the weak thermodynamic work of adhesion of PP/EPDM interface tends to block B-SiO_2 particles' transfer, thus making their temporary accumulation around EPDM particles. Here, these two factors provide the possibility for the formation of the filler-network structure from the thermodynamic angle. However, the kinetic control, mainly the use of the appropriate processing method and the controlling of the mixing time, plays a considerable role in the formation of the filler-network structure. More specifically, (3) for two-step processing method, in which SiO_2 particles are first dispersed in EPDM phase and then melt blend with PP matrix, the mixing time is sufficient for SiO_2 particles to migrate out from EPDM phase and finally pervade over the entire PP matrix. In these cases, the filler-network structure, as a relatively stable structure, is formed and frozen by crystallization of PP.

Acknowledgements

We would like to express our great thanks to the National Natural Science Foundation of China (50533050, 20490220, 20574081 and 50290090) for financial support. This work was subsidized by the special funds for Major State Basic Research Projects of China (2003CB615600) and by Ministry of Education of China as a key project (104154).

References

[1] Sahnoune F, Lopez Cuesta JM, Crespy A. Polym Eng Sci 2003;43:647.
[2] Gonzalez J, Albano C, Ichazo M, Diaz B. Eur Polym J 2002;38:2465.
[3] Thongruang W, Spontak RJ, Balik CM. Polymer 2002;43:3717.
[4] Gan DJ, Gao WJ, Song CS, Wang ZJ. Mater Lett 2001;51:120.
[5] Sung YT, Han MS, Song HK, Jung JW, Lee HS, Kum CK, et al. Polymer 2006;47:4434.
[6] Gubbels F, Jerome R, Teyssie Ph, Vanlathem E, Deltour R, Calderone A, et al. Macromolecules 1994;27:1972.
[7] Gubbels F, Blacher S, Vanlathem E, Jerome R, Deltour R, Brouers F, et al. Macromolecules 1995;28:1559.
[8] Gubbels F, Jerome R, Vanlathem E, Deltour R, Blacher S, Brouers F. Chem Mater 1998;10:1227.
[9] Shanks RA, Long Y. Polym Networks Blends 1997;7:87.
[10] Chang SQ, Xie TX, Yang GS. J Appl Polym Sci 2006;102:5184.
[11] Jancar J, Dibenedetto AT. J Mater Sci 1994;29:4651.
[12] Fisher I, Siegmann A, Narkis M. Polym Compos 2002;23:34.
[13] Hammer CO, Maurer FHJ, Molnar S, Pukanszky B. J Mater Sci 1999; 34:5911.
[14] Zhang L, Li CZ, Huang R. J Polym Sci 2005;43:1113.
[15] Prephet K, Horanont P. J Appl Polym Sci 2000;76:1929.
[16] Yang H, Zhang Q, Guo M, Wang C, Du RN, Fu Q. Polymer 2006;47: 2106.
[17] Pukanszky B, Tudos F, Kolarik J, Lednicky F. Polym Compos 1990; 11:98.
[18] Prephet K, Horanont P. Polymer 2000;41:9283.
[19] Hobbs SY, Dekkers MEJ, Watkins VH. Polymer 1998;29:1598.
[20] Guo HF, Gvozdic NV, Meier DJ. Polymer 1997;38:4915.
[21] Wu S. J Macromol Sci C Rev Macromol Chem 1974;10:1.
[22] Wu S. Polymer interface and adhesion. New York: Marcel Dekker; 1982.
[23] Wang Y, Zhang Q, Na B, Du RN, Fu Q, Shen KZ. Polymer 2003;44: 4261.
[24] Wu S. J Appl Polym Sci 1990;30:73.
[25] Wu S. Polymer 1985;26:1855.
[26] Wu S. J Appl Polym Sci 1988;35:549.
[27] Wu S. Polymer 1990;31:971.
[28] Margolina A, Wu S. Polymer 1988;29:2170.